Published in final edited form as:

*J Alzheimers Dis*. 2016 ; 51(2): 345–356. doi:10.3233/JAD-150859.

# The presence of select tau species in human peripheral tissues and their relation to Alzheimer's disease

**Brittany N. Dugger, PhD**[a,d,*], **Charisse M. Whiteside, BS**[a,d], **Chera L. Maarouf, BS**[a,d], **Douglas G. Walker, PhD**[a,d], **Thomas G. Beach, MD, PhD**[a,d], **Lucia I. Sue, BS**[a,d], **Angelica Garcia, BS**[a,d], **Travis Dunckley, PhD**[b,d], **Bessie Meechoovet**[b,d], **Eric M. Reiman, MD**[c,d], and **Alex E. Roher, MD,PhD**[a,d]

[a]Banner Sun Health Research Institute, Sun City, Arizona

[b]Translational Genomics Research Institute, Phoenix, Arizona

[c]Banner Alzheimer's Institute, Phoenix Arizona

[d]Arizona Alzheimer's Consortium

## Abstract

Tau becomes excessively phosphorylated in Alzheimer's disease (AD) and is widely studied within the brain. Further examination of the extent and types of tau present in peripheral tissues and their relation to AD is warranted given recent publications on pathologic spreading. Cases were selected based on the presence of pathological tau spinal cord deposits (N=18). Tissue samples from sigmoid colon, scalp, abdominal skin, liver, and submandibular gland were analyzed by Western blot and enzyme-linked immunosorbent assays (ELISAs) for certain tau species; frontal cortex gray matter was used for comparison. ELISAs revealed brain to have the highest total tau levels, followed by submandibular gland, sigmoid colon, liver, scalp, and abdominal skin. Western blots with antibodies recognizing tau phosphorylated at threonine 231(pT231), serine 396 and 404 (PHF-1), and an unmodified total human tau between residues 159 and 163 (HT7) revealed multiple banding patterns, some of which predominated in peripheral tissues. As submandibular gland had the highest levels of peripheral tau, a second set of submandibular gland samples were analyzed (N=36; 19 AD, 17 ND). ELISAs revealed significantly lower levels of pS396 (p=0.009) and pT231 (p=0.005) in AD cases but not total tau (p=0.18). Furthermore, pT231 levels in submandibular gland inversely correlated with Braak neurofibrillary tangle stage (p=0.04), after adjusting for age at death, gender, and post-mortem interval. These results provide evidence that certain tau species are present in peripheral tissues. Of potential importance, submandibular gland pT231 is progressively less abundant with increasing Braak neurofibrillary tangle stage.

[*]Corresponding Author, Brittany N. Dugger, PhD, c/o: University of California San Francisco, Institute for Neurodegenerative Diseases, 675 Nelson Rising Lane, NS 312, San Francisco, Ca 94143-0518, Phone: 415-502-6603, Fax: 415-476-8386, Brittany.dugger@ucsf.edu.

**Keywords**

propagation; spread; submandibular gland; colon; skin; liver; T231; HT7; PHF-1; Braak NFT stage

## Introduction

Tau is a microtubule-associated protein found in neuronal axons [1–3]. In the 1980's, tau was identified as a component of neurofibrillary tangles (NFTs), one of the abnormal protein deposits located within the brains of Alzheimer's disease (AD) cases [4, 5]. Subsequent research has shown that tau exists in adult humans in 6 isoforms generated by alternative splicing of three of the 16 exons (exons 2, 3, and 10) within tau mRNA [3]. The number and types of tau isoforms varies in a cell type specific manner and within different neurodegenerative diseases [2, 3, 6]. Tau proteins may also have a number of posttranslational modifications; in particular hyper-phosphorylation of tau at different positions, such as threonine 231 or serine 396 or 404, which are significantly increased in AD brains [3, 6–8].

In recent years, evidence from human pathology and experimental models has supported the concept that hallmark proteins of neurodegenerative diseases, including tau, may self-aggregate and spread via anatomical connectivity, perhaps through cell-to-cell transmission [9–11]. However, further studies are needed to show the extent and significance of this to disease pathogenesis. To understand the anatomic spread of tau, we recently conducted a comprehensive examination of the distribution of phosphorylated tau pathology in human spinal cords of ND and AD cases; and revealed tau pathology was present in over 95% of AD subjects and 50% of ND subjects [12]. Furthermore, there was a strong direct correlation between spinal cord tau deposits and Braak neurofibrillary tangle (NFT) stage, the main brain pathological staging scheme of AD. Given the spinal cord innervates all peripheral organs through autonomic and somatosensory nerve fibers, it appeared likely that pathological tau may also spread into the peripheral nervous system.

Investigations of tau species in peripheral tissue have mainly been restricted to rodents, with limited investigation of human tissues. A novel tau isoform with amino acids encoded by an additional 4a exon, giving the protein a molecular weight of 110kDa ("big tau") was identified in peripheral tissues [13] whereas in brain the main species of tau have molecular weights ranging from 45 to 65kDa [3, 13]. In the adult rat central nervous system, nearly all neurons that extend processes into the periphery express "big tau" [14]. Additionally, rat skeletal muscle, heart, testis, lung, and kidney contain relatively high levels of tau mRNA [15]. There have been investigations examining peripheral tau species in humans, but most have focused on one particular organ or used cultured fibroblasts [16–26]. Only one study, to our knowledge, examined tau deposits in humans in multiple organs, other than brain [17]. Using immunohistochemical methods with 10 normal controls and 24 AD subjects, 95 blocks from 21 different tissues were investigated; this study found curly fiber or tangle-like inclusions in 20/24 AD while these were absent in all controls in tissues such as the aorta, liver, spleen, and stomach [17].

Further examining the extent and type of peripheral tau in humans and its relation to AD may provide insights into patterns of tau aggregation and potential spreading in AD-related tauopathy beyond the brain. Furthermore, these investigations will provide additional insights into mechanisms and selective vulnerability of disease regardless of if there are correlations to brain pathology or not. The current study assesses the presence and levels of certain tau species, including native and phosphorylated forms in 5 peripheral areas (the sigmoid colon, liver, scalp, abdominal skin, and submandibular gland), in comparison to brain. The major finding from this study is that certain tau species have a decreased abundance in AD submandibular glands, and are inversely correlated with Braak NFT stage, a measure of pathological disease progression.

## Materials and Methods

### Tissue Samples

This study employed samples collected from elderly subjects who were participants in the BSHRI Brain and Body Donation Program (BBDP), a longitudinal clinicopathological study of normal aging, dementia and parkinsonism (website: www.brainandbodydonationprogram.org) [27, 28]. The BBDP has high quality tissue samples from brain as well as all major organs and tissues, from subjects with autopsy-confirmed neurodegenerative disease as well as age-similar control subjects. The operations of the BBDP and associated studies have been approved by the Banner Health Institutional Review Board, and all participants or next of kin gave informed consent for autopsy and tissue donation.

Two sets of samples were analyzed in this study. The details of these cases are described in Tables 1 and 2. For the first set of samples, the main goal was to determine the presence or absence of tau within several peripheral sites (the sigmoid colon, liver, scalp, abdominal skin, and submandibular gland). To enhance the probability of detecting tau in peripheral tissues, cases which were known to contain phosphorylated tau deposits in all areas of their spinal cords were utilized (Table 1) [12]. For the second set of samples, the purpose was to determine the relationship of submandibular gland tau to AD and Braak NFT stage, and cases were chosen accordingly (Table 2). Braak NFT stages were grouped (Braak 0-II, Braak III-IV, and Braak V-VI) due to the low abundance of certain Braak NFT stages within our BBDP.

### Tissue preparation for biochemical analyses

At the time of autopsy tissue specimens were frozen on dry ice and stored at −80°C. Frozen specimens (approx. 500 mg) from liver, sigmoid colon, scalp, submandibular gland, abdominal skin, and gray matter of the middle frontal gyrus of selected cases were dissected on dry ice. Tissue was processed according to previously published methods [29]. In brief, samples were homogenized in 2mL of 90% glass-distilled formic acid (GDFA) using an Omni tissue grinder and plastic probes, then centrifuged at 200,000 x g in a Beckman 50.4Ti at 200,000 x g for one hour. The supernatant of each sample was removed and stored at −80°C, subsequently, the supernatant was dialyzed with deionized water (3 changes, 30 min each) then with 0.1 M ammonium carbonate (2 changes, 1 h each) using 1000 Molecular

Weight Cut Off (MWCO) dialysis tubing. Samples were then flash frozen in a dry ice/ethanol bath and lyophilized for 48 hours.

For ELISAs, each lyophilized sample was reconstituted in 500 μl 5 M guanidine hydrochloride (GHCl), 50 mM Tris-HCl, pH 8.0, containing protease and phosphatase inhibitors (Thermo Fisher Scientific, Grand Island, NY), then centrifuged at 435,000 × g in a Beckman TLA 120.2 rotor for 20 min). The supernatant was employed in ELISA assays following measurement of total protein concentration determined with Pierce's Micro BCA protein assay kit (Thermo Fisher Scientific). Lyophilized samples to be analyzed by Western blotting were dissolved in 5% SDS, 5 mM EDTA, 20 mM Tris-HCl, pH 7.8 containing protease and phosphatase inhibitors (Thermo Fisher Scientific).

## Western blot analyses

A total of 30 μg protein/sample for peripheral tissues and 1 μg protein/sample of brain were used for Western blots using Novex NUPAGE Bis-Tris 4–12% gel system according to manufacturer's protocols (Thermo Fisher Scientific) These methods have been previously described [29, 30]. After transfer onto Nitrocellulose Pre-Cut Blotting Membranes, 0.45 μm pore size (Thermo Fisher Scientific), membranes were blocked for 1 hour with a 5% milk solution in PBS with 0.05% Tween 20 (PBS-T). Primary and secondary antibodies were diluted in the same buffer. Primary antibody incubation was carried out at 4°C for approximately 18 hours. The primary antibodies were monoclonal anti-mouse antibody recognizing normal human tau between residues 159 and 163: HT7 (dilution 1:1000, Thermo Fisher Scientific), a rabbit monoclonal to phosphorylated tau at Threonine 231:pT231 (dilution 1:1000 Abcam, Cambridge, MA), and a mouse monoclonal to tau phosphorylated at serine 396 and 404: PHF-1 (dilution 1:1000, a gift from Peter Davies). To detect bound antibodies, membranes were washed 3 times at 5 minutes each in PBS-T, then incubated at room temperature for 2 hours in appropriate horseradish peroxidase (HRP) conjugated secondary antibodies: goat anti-mouse IgG (1:10,000 Thermo Fisher Scientific) or donkey anti-rabbit IgG (1:1000, Thermo Fisher Scientific). The blots were then washed twice with PBS-T, with a final wash in PBS then developed using a horseradish peroxidase chemiluminescent substrate (Western bright Quantum HRP kit, Advansta, Menlo Park, CA) and imaged with an Alpha Innotech FlourochemQ Multiimager II. After initial imaging, the membranes were washed, boiled in phosphate-buffered saline for 2 minutes, re-blocked, and re-probed with a monoclonal anti-mouse to GAPDH (dilution 1:100,000 Thermo Fisher Scientific) to normalize protein levels.

## Peptide Absorption

Given that certain banding patterns with the HT7 antibody were not predominant in brain samples, to confirm specificity, a subsequent membrane was incubated with HT7 primary antibody containing 10x the concentration (ug/uL) of a blocking peptide that was synthesized at the Koch Institute (Massachusetts Institute of Technology, Boston MA) containing the epitope recognized by HT7 (PPGQK with capped ends (N-terminal CH3CONH, C-terminal CONH2)). All other procedures were completed as described above. Furthermore, we performed similar methods for immunohistochemistry, incubating

formalin-fixed paraffin-embedded (FFPE) sections with HT7 primary antibody containing 10x the concentration of the blocking peptide.

## ELISA analyses

The levels of total tau in peripheral organs tissues were measured by enzyme-linked immunosorbent assay (ELISA) Kits (Thermo Fisher Scientific), following the manufacturer's instructions. For the second series of submandibular glands, total tau (Thermo Fisher Scientific), and levels of phosphorylated tau detected by pT231 (Thermo Fisher Scientific) and pS396 (Thermo Fisher Scientific) were quantified. All steps were performed at room temperature. Optical density of each well was measured immediately after adding Stop Solution using a plate reader set at an absorbance of 450 nm for 1 second; sample concentrations were calculated against the generated standard curves. Total tau and S396 data were then adjusted to ng tau/mg sample protein, while T231 data were adjusted to T231 units/mg sample protein.

## Immunohistochemistry

Tissue processing methods and neuropathological assessment have been previously described [27, 28]. Five micron formalin-fixed paraffin-embedded (FFPE) sections of submandibular gland were immunohistochemically stained with the same antibodies utilized for western blot: HT7, pT231, and PHF-1 using immunoperoxidase methods. All FFPE sections were deparaffinized in clearing agents followed by rehydration in a graded series of alcohols. For HT7 and PHF-1 antibodies, deparaffinized sections were then immersed in $dH_2O$, while T231 slides were immersed in citrate buffer (pH 6.0). All slides were then subsequently subjected to 15 minutes of indirect steam for antigen retrieval. After steam, slides were brought to room temperature through displacement with $dH_2O$. All slides were then incubated in 1% $H_2O_2$, for 30 minutes to quench endogenous peroxidases, then washed in PBS-T three times for 5 minutes each, and incubated overnight at 4*C in their respective antibody. The following day, sections were incubated in their appropriate secondary antibodies for 2 hours then subjected to ABC complex (VECTASTAIN® ABC systems, Vector Laboratories Catalog #s PK-6102 for mouse IgG, and PK6101 for Rabbit IgG) for 30 minutes and rinsed 2 times in PBS-T for 5minutes, and then in Tris buffer for 5 minutes. All sections were then developed with nickel-enhanced 3, 3′-diaminobenzidine (DAB) as the chromogen and counterstained with Neutral Red.

## Statistical analysis

All statistical analyses were performed with Sigma Plot 12.0 (Systat Software, Inc., San Jose, CA, USA). Given there were only 2 ND within the first group, no statistical analyses comparing ND to AD were conducted. For demographic data for the second series of tissues, group means were compared using Mann-Whitney U-tests. Gender ratios were compared using chi-squared tests. Pearson product moment correlations were used to note the relationships between ELISA tau levels (pT231, pS396, and total tau) in the submandibular gland to age at death, PMI, and gender. Given there were statistically significant associations of ELISA data to certain demographic variables (age at death and PMI) and there have been reports of gender differences for peripheral tau [21], linear regression analysis for the relationship of ELISA results (pT231, pS396, and total tau) to AD status and grouped Braak

NFT stage were adjusted for age at death, post-mortem interval (PMI), and gender. The significance level for all tests was set at $p < 0.05$.

## Results

For the initial comparison of different peripheral tissues (N=18), average age at death was 84.7 ± 5.28 years, average postmortem interval was 3.8 ± 2.52 hours, and male to female ratio was 9:9 for the series. Average disease duration for the AD cases was 8.3 ± 4.82 years (Table 1). For the extended investigation of submandibular gland tissues (Table 2), average age at death for the entire series was 80.9 ± 12.79 years; average postmortem interval was 3.3 ± 1.81 hours, and male to female ratio was 24:12. Average disease duration for the AD group was 7.4 ± 7.71 years. For AD (N=19), average age was 84.1± 6.93 years, PMI was 3.3±1.07 hours, and M: F ratio was 13:6. For ND (N=17) average age was 77.3±16.68 years, PMI was 3.4±2.42 hours, and M: F ratio was 11:6. There were no differences in the submandibular gland series among AD/ND or grouped Braak NFT stages with respect to postmortem interval, male to female ratios, or age at death. As expected, there were significant differences on the frequency of a clinicopathological diagnosis of AD within each grouped Braak NFT stage.

### Presence of tau in peripheral tissues

The different forms of unmodified tau in peripheral tissues were detected using the antibody HT7 [29]. The most prominent HT7 band in all peripheral tissues was at a molecular weight corresponding to 31kDa, but this band was not prominent in AD or ND brain tissues (Figure 1 A) even after longer exposures. Another band of approximately 25kDa, was present in select organs (liver, submandibular gland, and colon). The tau immunoreactive bands of 45–60 kDa in AD and ND brains were also present in the submandibular gland and colon samples, while only a single band of approximately 60 kDa was present in skin samples A tau reactive band of approximately 110 kDa was detectable only in the submandibular gland and colon, even after longer exposures. All immunoreactive bands were absent when HT7 antibody was pre-absorbed with a peptide specific for the epitope (Figure 2). These analyses were followed up using antibodies specific for phosphorylated forms of tau (Figure 1 B-C). Using the PHF-1 antibody, there was a low abundance band of approximately 60kDa in select organs (submandibular gland, colon, and abdominal skin; Figure 1 B). A band of approximately 60kDa molecular weight was detected with the pT231 antibody that was most prominent in the submandibular gland and brain. In the liver and submandibular gland, there was also a pT231 band of approximately 45 kDa and this was also presence in low abundance in colon and abdominal skin (between the 31 and 60 kDa marker- Figure 1 C).

### Quantitative measures of tau

Total tau levels in peripheral tissues were measured using ELISAs. Total tau levels in gray matter of the middle frontal gyrus were 7889±2742ng/mg (average± standard deviation for both AD and ND) with an average of 7941±237 ng/mg total protein for ND (N=2) and 7882±2945 ng/mg total protein for AD (N=16). Levels in peripheral tissues were, for submandibular gland 120±25.9ng/mg (136ng/mg ND, 117ng/mg AD), sigmoid colon 22±9.0ng/mg (21ng/mg ND, 22ng/mg AD), liver 13±4.6ng/mg (12ng/mg ND, 19ng/mg

AD), scalp 14±5.7ng/mg (19ng/mg ND, 14ng/mg AD), and abdominal skin 21±16.1ng/mg (10ng/mg ND, 20ng/mg AD) (Figure 3). These values ranged from 1.72% of in the submandibular gland (i.e. total tau of submandibular gland/brain) to 0.16% in the liver (Table 3).

### Submandibular gland tau in relation to grouped Braak NFT stages

Representative images of Western blots of submandibular gland tissues with progressively increasing Braak NFT stages are shown in Figure 4. All submandibular gland tissues contained similar banding patterns, as described above. ELISAs for total and phosphorylated tau were carried out to determine if there were differences between AD submandibular gland tau levels as compared to ND cases. After adjusting for PMI, age at death, and gender, the submandibular glands of AD cases had significantly lower levels of pT231 ($R^2$=0.38, p=0.005) and pS396 ($R^2$=0.274, p=0.009), while there were no significant differences with respect to total tau ($R^2$=0.208, p=0.18) (Figure 5). Additionally, there were significantly lower pT231 levels ($R^2$=0.29, p=0.044) with increasing grouped Braak NFT stage (Figure 6) while this relationship was close to significance with total tau ($R^2$=0.261, p=0.051) and absent with pS396 ($R^2$=0.149, p=0.162) (Figure 6). There were also significant relationships with increased age after adjustment for PMI, gender, and AD status for pT231 (p=0.029) but not for pS396 (p=0.058) or total tau (p=0.114). Furthermore, pT231 levels (p=0.023), but not pS396 (p=0.118) or total tau (p=0.644) levels, were significantly and inversely correlated with PMI.

For correlations amongst levels of individual tau species, analyzing both ND and AD together, there were significant direct associations among both phosphorylated species pS396 and pT231 (Pearson product moment=0.697, p <0.0001) and between pT231 and total tau levels (Pearson product moment=0.423, p=0.013). There was no significant relationship between pS396 and total tau (Pearson product moment= 0.127, p=0.469).

### Immunohistochemistry

Initial immunohistochemistry staining of 5 μm FFPE submandibular gland tissues for HT7 revealed immunoreactivity within stromal nerve fascicles, ganglion cells, nerve fibers, and diffuse staining of simple cuboidal epithelial cells lining secretory ducts in both AD and ND cases (representative photos Figure 7 A-D, and Figure 8 A). Immunohistochemistry with T231 (Figure 7 E-H) and PHF-1 (Figure 7 I-L) revealed similar immunoreactive patterns, however, T231 and PHF-1 did not demonstrate immunoreactivity within simple cuboidal epithelial cells. With respect to HT7 specificity, nearly all immunoreactivity was absent (figure 8 B) when the HT7 antibody was pre-absorbed with a peptide specific for the epitope.

## Discussion

Recent work has indicated a potential for cell-to-cell transmission of abnormally aggregated proteins such as tau [9–11, 31–34]. In the human brain, the presence of pathological tau in neuroanatomically connected brain regions has long suggested a physical spread of disease scheme [35, 36]. Our previous work demonstrated that pathological tau spreads beyond the

brain into the spinal cord, with a rostral to caudal gradient and is progressively greater with increased Braak NFT stage [12]. The current study demonstrates that certain tau species can be detected, although at levels much lower than those found in brain, in samples from the sigmoid colon, scalp, abdominal skin, liver, and submandibular gland. Furthermore, these results support that a physical spread of brain pathologic tau forms may not perhaps be extended into the periphery, at least for the submandibular gland. Further exploration of this could enhance knowledge of the molecular underpinnings of why tau aggregates within certain anatomic regions. In the submandibular gland, AD cases had lower levels of phosphorylated forms of tau (pT231 and pS396) when compared to ND and there were lower levels of certain tau species as Braak NFT stages increased.

Prior investigations have examined peripheral tau in normal and diseased humans, and few studies have been published in relation to AD [16–23]. Tau aggregates are found in inclusion body myositis [20], tau levels have been linked to drug resistance in some forms of cancer [22, 23], and tau gene expression in male skin has been shown to be significantly increased with age [21]. In reference to AD, in a single study, pathological tau deposits were reportedly present in numerous peripheral organs, such as the aorta, liver, spleen, and stomach, of AD subjects but not controls [17]. There have been published rodent studies demonstrating big tau to be the predominant form in peripheral tissues [3, 13]. Our results confirm the presence of big tau in certain human tissues and revealed additional lower molecular weight peripheral tau species.

Within the submandibular gland, which contained the highest total tau levels of all peripheral tissues examined, the results are surprising in that AD cases had significantly lower, rather than higher, levels of phosphorylated forms of tau (pT231 and pS396) while for total tau this difference was near the significance level ($p=0.051$). Lower levels of phosphorylated and total tau in AD submandibular glands may seem at first to be counterintuitive. One possibility is that the presence of pathological forms of tau causes a “dying-back” neuropathy with resultant lowers axonal density and hence tau levels. Further investigations of other axonal proteins are warranted. The ubiquitous presence, within peripheral axons, of abnormally phosphorylated tau forms that are restricted within the central nervous system to subjects with AD, is puzzling. Other evidence indicates that the submandibular gland may be a potentially fruitful area for AD investigations. Tau mRNA has been reported to be highly expressed in salivary glands [37]. The submandibular gland is innervated by parasympathetic fibers carried by the facial nerve and by preganglionic and postganglionic sympathetic fibers originating from the thoracic spinal cord and cervical sympathetic ganglia, respectively [38, 39]. Functionally, the submandibular gland produces most of the salivary volume, and saliva flow rates have been shown to be significantly lower in AD patients when compared to controls [26]. A recent study examining saliva demonstrated the phosphorylated tau/total tau ratio to be significantly increased in patients with AD compared to healthy controls [19]. Although tau species may be increased in saliva, the decreased saliva flow rates in AD may be due to a regressive neuropathy.

Our previous investigations on the peripheral distribution of pathological alpha-synuclein in Lewy body diseases indicates that a neurodegenerative proteinopathy can spread widely throughout the peripheral nervous system, and that the submandibular gland is amongst the

most affected peripheral sites [40, 41]. The current results of lower peripheral tau levels in submandibular gland and other peripheral sites from AD as compared to ND cases, do not, on the surface, support a spread of AD-related tau pathology beyond the central nervous system. The differences in disease-related abundance between peripheral tau and alpha-synuclein suggests that each proteinopathy may have a different propensity, neuronal-specific vulnerability and/or mode of peripheral spread, just as their central nervous system neuroanatomical distribution patterns differ [35, 42, 43].

There are numerous hypotheses on how different forms of tau have specific aggregation propensity or associations with selective vulnerability. Tau forms identified by antibodies to pT231 label early AD brain pathological stages known as pre-tangles, while late-stage AD extracellular tangles are labeled with PHF-1; although these data may be dependent on methods utilized [44]. PHF-1 demonstrated only very weak Western blot bands in peripheral tissues which were detected only after very long exposures. It is possible, however, that this may have been due to tissue processing methods that may not have permitted the complete solubilization of the PHF-1 reactive tau [45, 46]. This was not the case with pT231, which demonstrated intense low molecular weight bands within peripheral tissues. These potential tau molecular differences between central and peripheral nervous system may provide additional insights into selective vulnerability.

## Acknowledgements:

The authors would like to thank the families and participants of the BBDP for their generous donations. The author would also like to thank the laboratory of Dr. Paul Coleman for the use of equipment to conduct these studies. This study was funded by the Sun Health Foundation and the Arizona Department of Health Services through a grant from the Arizona Alzheimer's Research Consortium. The Brain and Body Donation Program at Banner Sun Health Research Institute has received support from the National Institute of Neurological Disorders and Stroke (U24 NS072026 National Brain and Tissue Resource for Parkinson's Disease and Related Disorders), the National Institute on Aging (P30 AG19610 Arizona Alzheimer's Disease Core Center), the Arizona Department of Health Services (contract 211002, Arizona Alzheimer's Research Center), the Arizona Biomedical Research Commission (contracts 4001, 0011, 05–901 and 1001 to the Arizona Parkinson's Disease Consortium) and the Michael J. Fox Foundation for Parkinson's Research.

## References

[1]. Binder LI , Frankfurter A , Rebhun LI (1985) The distribution of tau in the mammalian central nervous system. J Cell Biol 101, 1371–1378.3930508

[2]. Mandelkow EM , Mandelkow E (2012) Biochemistry and cell biology of tau protein in neurofibrillary degeneration. Cold Spring Harb Perspect Med 2, a006247.22762014

[3]. Buee L , Bussiere T , Buee-Scherrer V , Delacourte A , Hof PR (2000) Tau protein isoforms, phosphorylation and role in neurodegenerative disorders. Brain Res Brain Res Rev 33, 95–130.10967355

[4]. Brion JP , Couck AM , Passareiro E , Flament-Durand J (1985) Neurofibrillary tangles of Alzheimer's disease: an immunohistochemical study. J Submicrosc Cytol 17, 89–96.3973960

[5]. Grundke-Iqbal I , Iqbal K , Tung YC , Quinlan M , Wisniewski HM , Binder LI (1986) Abnormal phosphorylation of the microtubule-associated protein tau (tau) in Alzheimer cytoskeletal pathology. Proc Natl Acad Sci U S A 83, 4913–4917.3088567

[6]. Andreadis A (2005) Tau gene alternative splicing: expression patterns, regulation and modulation of function in normal brain and neurodegenerative diseases. Biochim Biophys Acta 1739, 91–103.15615629

[7]. Yoshida M (2006) Cellular tau pathology and immunohistochemical study of tau isoforms in sporadic tauopathies. Neuropathology 26, 457–470.17080726

[8]. Tolnay M , Probst A (1999) REVIEW: tau protein pathology in Alzheimer's disease and related disorders. Neuropathol Appl Neurobiol 25, 171–187.10417659

[9]. Goedert M , Falcon B , Clavaguera F , Tolnay M (2014) Prion-like mechanisms in the pathogenesis of tauopathies and synucleinopathies. Curr Neurol Neurosci Rep 14, 495.25218483

[10]. Luk KC , Kehm V , Carroll J , Zhang B , O'Brien P , Trojanowski JQ , Lee VM (2012) Pathological alpha-synuclein transmission initiates Parkinson-like neurodegeneration in nontransgenic mice. Science 338, 949–953.23161999

[11]. Ahmed Z , Cooper J , Murray TK , Garn K , McNaughton E , Clarke H , Parhizkar S , Ward MA , Cavallini A , Jackson S , Bose S , Clavaguera F , Tolnay M , Lavenir I , Goedert M , Hutton ML , O'Neill MJ (2014) A novel in vivo model of tau propagation with rapid and progressive neurofibrillary tangle pathology: the pattern of spread is determined by connectivity, not proximity. Acta Neuropathol 127, 667–683.24531916

[12]. Dugger BN , Hidalgo JA , Chiarolanza G , Mariner M , Henry-Watson J , Sue LI , Beach TG (2013) The distribution of phosphorylated tau in spinal cords of Alzheimer's disease and non-demented individuals. J Alzheimers Dis 34, 529–536.23246918

[13]. Goedert M , Spillantini MG , Crowther RA (1992) Cloning of a big tau microtubule-associated protein characteristic of the peripheral nervous system. Proc Natl Acad Sci U S A 89, 1983–1987.1542696

[14]. Boyne LJ , Tessler A , Murray M , Fischer I (1995) Distribution of Big tau in the central nervous system of the adult and developing rat. J Comp Neurol 358, 279–293.7560287

[15]. Gu Y , Oyama F , Ihara Y (1996) Tau is widely expressed in rat tissues. J Neurochem 67, 1235–1244.8752131

[16]. Miklossy J , Qing H , Radenovic A , Kis A , Vileno B , Laszlo F , Miller L , Martins RN , Waeber G , Mooser V , Bosman F , Khalili K , Darbinian N , McGeer PL (2010) Beta amyloid and hyperphosphorylated tau deposits in the pancreas in type 2 diabetes. Neurobiol Aging 31, 1503–1515.18950899

[17]. Miklossy J , Taddei K , Martins R , Escher G , Kraftsik R , Pillevuit O , Lepori D , Campiche M (1999) Alzheimer disease: curly fibers and tangles in organs other than brain. J Neuropathol Exp Neurol 58, 803–814.10446805

[18]. Hattori H , Matsumoto M , Iwai K , Tsuchiya H , Miyauchi E , Takasaki M , Kamino K , Munehira J , Kimura Y , Kawanishi K , Hoshino T , Murai H , Ogata H , Maruyama H , Yoshida H (2002) The tau protein of oral epithelium increases in Alzheimer's disease. J Gerontol A Biol Sci Med Sci 57, M64–70.11773216

[19]. Shi M , Sui YT , Peskind ER , Li G , Hwang H , Devic I , Ginghina C , Edgar JS , Pan C , Goodlett DR , Furay AR , Gonzalez-Cuyar LF , Zhang J (2011) Salivary tau species are potential biomarkers of Alzheimer's disease. J Alzheimers Dis 27, 299–305.21841250

[20]. Askanas V , Engel WK (2008) Inclusion-body myositis: muscle-fiber molecular pathology and possible pathogenic significance of its similarity to Alzheimer's and Parkinson's disease brains. Acta Neuropathol 116, 583–595.18974994

[21]. Makrantonaki E , Brink TC , Zampeli V , Elewa RM , Mlody B , Hossini AM , Hermes B , Krause U , Knolle J , Abdallah M , Adjaye J , Zouboulis CC (2012) Identification of biomarkers of human skin ageing in both genders. Wnt signalling - a label of skin ageing? PLoS One 7, e50393.23226273

[22]. Rouzier R , Rajan R , Wagner P , Hess KR , Gold DL , Stec J , Ayers M , Ross JS , Zhang P , Buchholz TA , Kuerer H , Green M , Arun B , Hortobagyi GN , Symmans WF , Pusztai L (2005) Microtubule-associated protein tau: a marker of paclitaxel sensitivity in breast cancer. Proc Natl Acad Sci U S A 102, 8315–8320.15914550

[23]. Souter S , Lee G (2009) Microtubule-associated protein tau in human prostate cancer cells: isoforms, phosphorylation, and interactions. J Cell Biochem 108, 555–564.19681044

[24]. Ingelson M , Vanmechelen E , Lannfelt L (1996) Microtubule-associated protein tau in human fibroblasts with the Swedish Alzheimer mutation. Neurosci Lett 220, 9–12.8977136

[25]. Francois M , Leifert W , Martins R , Thomas P , Fenech M (2014) Biomarkers of Alzheimer's disease risk in peripheral tissues; focus on buccal cells. Curr Alzheimer Res 11, 519–531.24938500

[26]. Ship JA , DeCarli C , Friedland RP , Baum BJ (1990) Diminished submandibular salivary flow in dementia of the Alzheimer type. J Gerontol 45, M61–66.2313044

[27]. Beach TG , Sue LI , Walker DG , Roher AE , Lue L , Vedders L , Connor DJ , Sabbagh MN , Rogers J (2008) The Sun Health Research Institute Brain Donation Program: description and experience, 1987–2007. Cell Tissue Bank 9, 229–245.18347928

[28]. Beach TG , Adler CH , Sue LI , Serrano G , Shill HA , Walker DG , Lue L , Roher AE , Dugger BN , Maarouf C , Birdsill AC , Intorcia A , Saxon-Labelle M , Pullen J , Scroggins A , Filon J , Scott S , Hoffman B , Garcia A , Caviness JN , Hentz JG , Driver-Dunckley E , Jacobson SA , Davis KJ , Belden CM , Long KE , Malek-Ahmadi M , Powell JJ , Gale LD , Nicholson LR , Caselli RJ , Woodruff BK , Rapscak SZ , Ahern GL , Shi J , Burke AD , Reiman EM , Sabbagh MN (2015) Arizona Study of Aging and Neurodegenerative Disorders and Brain and Body Donation Program. Neuropathology.

[29]. Maarouf CL , Daugs ID , Kokjohn TA , Walker DG , Hunter JM , Kruchowsky JC , Woltjer R , Kaye J , Castano EM , Sabbagh MN , Beach TG , Roher AE (2011) Alzheimer's disease and non-demented high pathology control nonagenarians: comparing and contrasting the biochemistry of cognitively successful aging. PLoS One 6, e27291.22087282

[30]. Maarouf CL , Beach TG , Adler CH , Malek-Ahmadi M , Kokjohn TA , Dugger BN , Walker DG , Shill HA , Jacobson SA , Sabbagh MN , Roher AE (2013) Quantitative appraisal of ventricular cerebrospinal fluid biomarkers in neuropathologically diagnosed Parkinson's disease cases lacking Alzheimer's disease pathology. Biomark Insights 8, 19–28.23533154

[31]. Sanders DW , Kaufman SK , DeVos SL , Sharma AM , Mirbaha H , Li A , Barker SJ , Foley AC , Thorpe JR , Serpell LC , Miller TM , Grinberg LT , Seeley WW , Diamond MI (2014) Distinct tau prion strains propagate in cells and mice and define different tauopathies. Neuron 82, 1271–1288.24857020

[32]. Clavaguera F , Bolmont T , Crowther RA , Abramowski D , Frank S , Probst A , Fraser G , Stalder AK , Beibel M , Staufenbiel M , Jucker M , Goedert M , Tolnay M (2009) Transmission and spreading of tauopathy in transgenic mouse brain. Nat Cell Biol 11, 909–913.19503072

[33]. Jucker M , Walker LC (2013) Self-propagation of pathogenic protein aggregates in neurodegenerative diseases. Nature 501, 45–51.24005412

[34]. Clavaguera F , Hench J , Goedert M , Tolnay M (2015) Invited review: Prion-like transmission and spreading of tau pathology. Neuropathol Appl Neurobiol 41, 47–58.25399729

[35]. Braak H , Braak E (1991) Neuropathological stageing of Alzheimer-related changes. Acta Neuropathol 82, 239–259.1759558

[36]. Pearson RC , Esiri MM , Hiorns RW , Wilcock GK , Powell TP (1985) Anatomical correlates of the distribution of the pathological changes in the neocortex in Alzheimer disease. Proc Natl Acad Sci U S A 82, 4531–4534.3859874

[37]. Conrad C , Vianna C , Freeman M , Davies P (2002) A polymorphic gene nested within an intron of the tau gene: implications for Alzheimer's disease. Proc Natl Acad Sci U S A 99, 7751–7756.12032355

[38]. Bailey BJ , Johnson JT (2006) Head and Neck Surgery-Otolaryngology, Lippincott Williams & Wilkins, Philadelphia, PA.

[39]. Ferreira JN , Hoffman MP (2013) Interactions between developing nerves and salivary glands. Organogenesis 9, 199–205.23974175

[40]. Adler CH , Dugger BN , Hinni ML , Lott DG , Driver-Dunckley E , Hidalgo J , Henry-Watson J , Serrano G , Sue LI , Nagel T , Duffy A , Shill HA , Akiyama H , Walker DG , Beach TG (2014) Submandibular gland needle biopsy for the diagnosis of Parkinson disease. Neurology 82, 858–864.24500652

[41]. Beach TG , Adler CH , Dugger BN , Serrano G , Hidalgo J , Henry-Watson J , Shill HA , Sue LI , Sabbagh MN , Akiyama H (2013) Submandibular gland biopsy for the diagnosis of Parkinson disease. J Neuropathol Exp Neurol 72, 130–136.23334596

[42]. Kosaka K , Yoshimura M , Ikeda K , Budka H (1984) Diffuse type of Lewy body disease: progressive dementia with abundant cortical Lewy bodies and senile changes of varying degree--a new disease? Clin Neuropathol 3, 185–192.6094067

[43]. Beach TG , Adler CH , Lue L , Sue LI , Bachalakuri J , Henry-Watson J , Sasse J , Boyer S , Shirohi S , Brooks R , Eschbacher J , White CL , 3rd, Akiyama H, Caviness J, Shill HA, Connor DJ, Sabbagh MN, Walker DG (2009) Unified staging system for Lewy body disorders: correlation with nigrostriatal degeneration, cognitive impairment and motor dysfunction. Acta Neuropathol 117, 613–634.19399512

[44]. Augustinack JC , Schneider A , Mandelkow EM , Hyman BT (2002) Specific tau phosphorylation sites correlate with severity of neuronal cytopathology in Alzheimer's disease. Acta Neuropathol 103, 26–35.11837744

[45]. Smith MA , Nagaraj RH , Perry G (1997) Protocol for quantitative analysis of paired helical filament solubilization: a method applicable to insoluble amyloids and inclusion bodies. Brain Res Brain Res Protoc 1, 247–252.9385061

[46]. Iqbal K , Zaidi T , Thompson CH , Merz PA , Wisniewski HM (1984) Alzheimer paired helical filaments: bulk isolation, solubility, and protein composition. Acta Neuropathol 62, 167–177.6538056

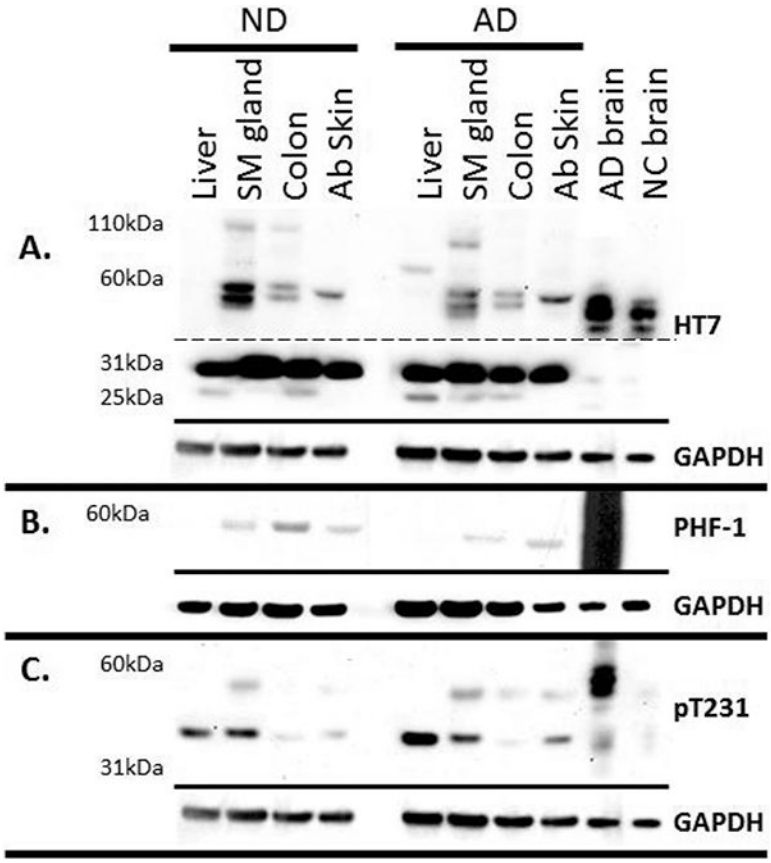


**Figure 1.**

Tau Western blots of a non-demented control (ND) and an Alzheimer's disease (AD) case. 30ug of peripheral organ and 1ug of brain were run on 4–12% Bis-Tris gels and probed with A) HT7 (dashed line indicates different exposure times: Top long exposure, bottom short exposure), B) PHF-1 and C) T231. GAPDH was used as a protein loading control, and is located below each blot. Scalp was not included due to extremely low protein concentration determined by BCA assay.

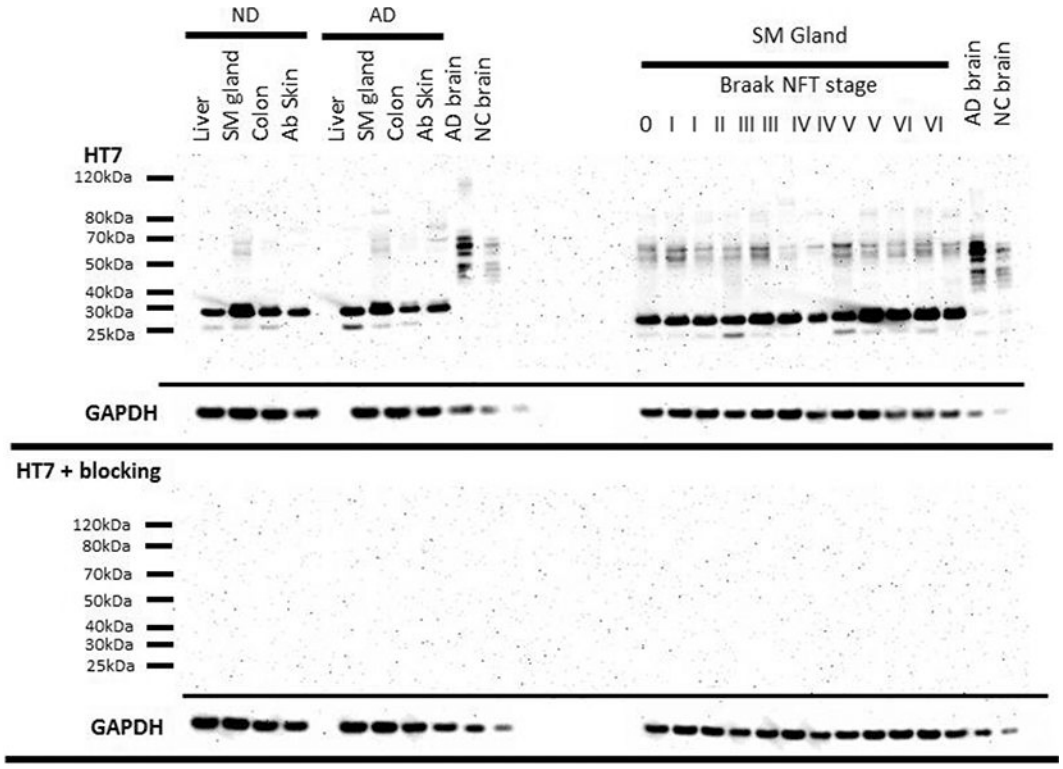


**Figure 2.**

Tau Western blots of peripheral organs (left) and submandibular gland tissues from a variety of Braak NFT stages (right) of 30ug of tissue and 1ug of brain probed with a HT7 (top) and probed with HT7 and a blocking peptide (10x the concentration of HT7) directed towards the HT7 sequence. Boxes below each respective blot represent GAPDH of that blot.

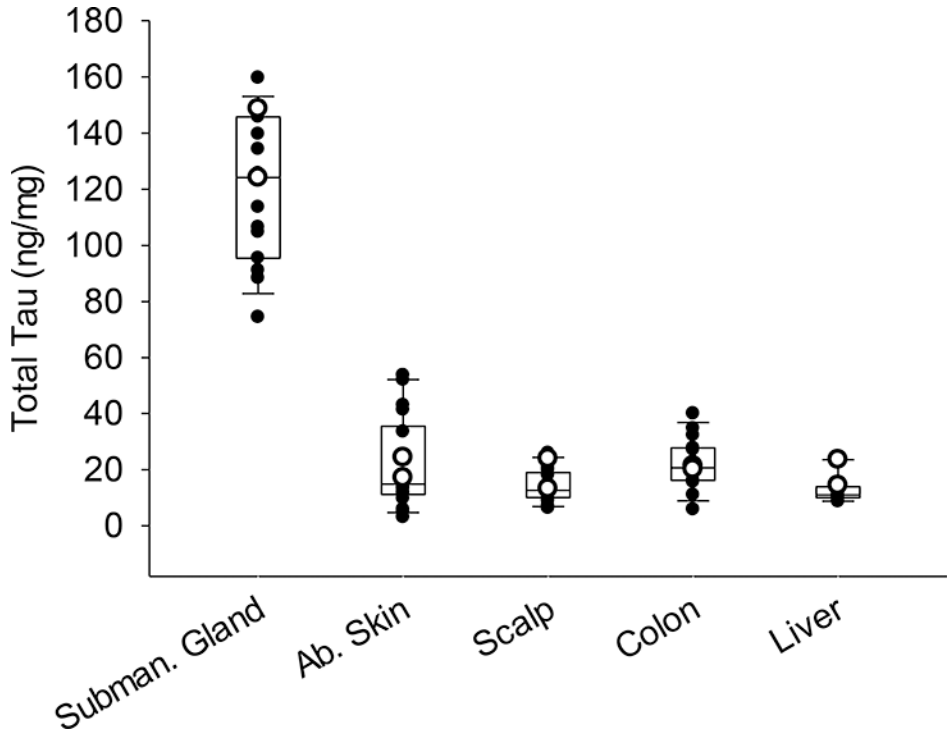


**Figure 3.**

Box and whisker plots with overlaying dot plots of ELISA measures of total tau in peripheral tissues of 18 cases (white dots = ND and black dots= AD cases). The bottom and top of the boxes represent the first and third quartiles, respectively; and the band inside the box is the median value. mg refers to mg of total protein.

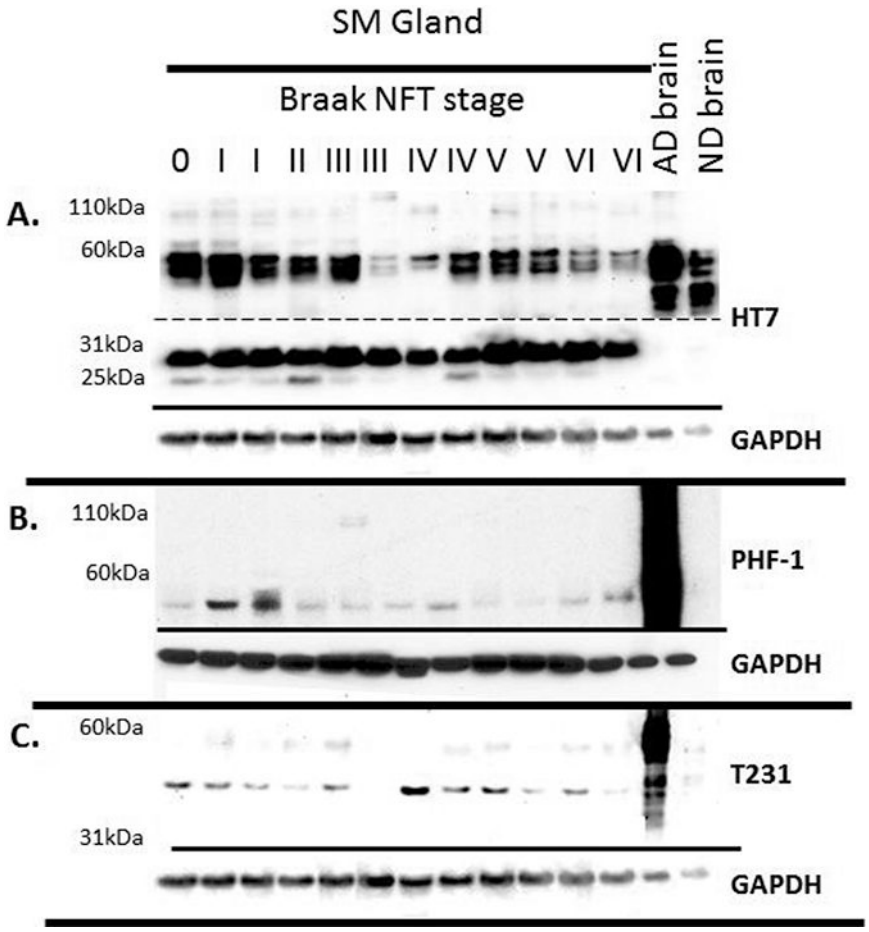


**Figure 4.**

Tau Western blots of submandibular gland tissues from a variety of Braak NFT stages. 30ug of submandibular gland and 1ug of brain were run on 4–12% Bis-Tris gels and probed with A) HT7 (dashed line indicates different exposure times: Top long exposure, bottom short exposure), B) PHF-1, C) and T231. GAPDH was used as a protein loading control and is located below each blot.

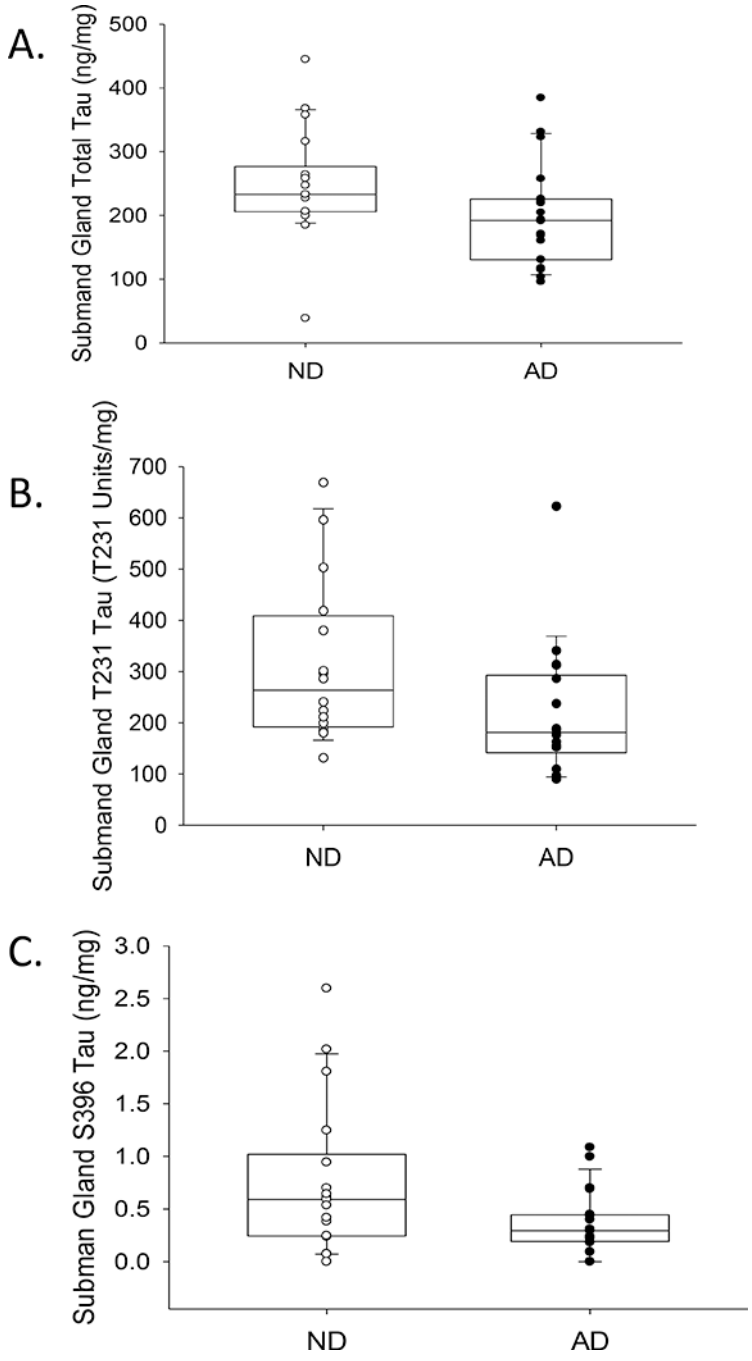


**Figure 5.**

Box and whisker plots with overlaying dot plots of ELISA measures of A) total, B) T231 and C) S396 tau species in submandibular glands of AD and ND cases. When adjusting for age, PMI, and gender there were significant differences with T231 (p=0.005) and S396 (p=0.009) a marginal difference with total tau levels (p=0.051) based on presence of AD. mg refers to mg of total protein.

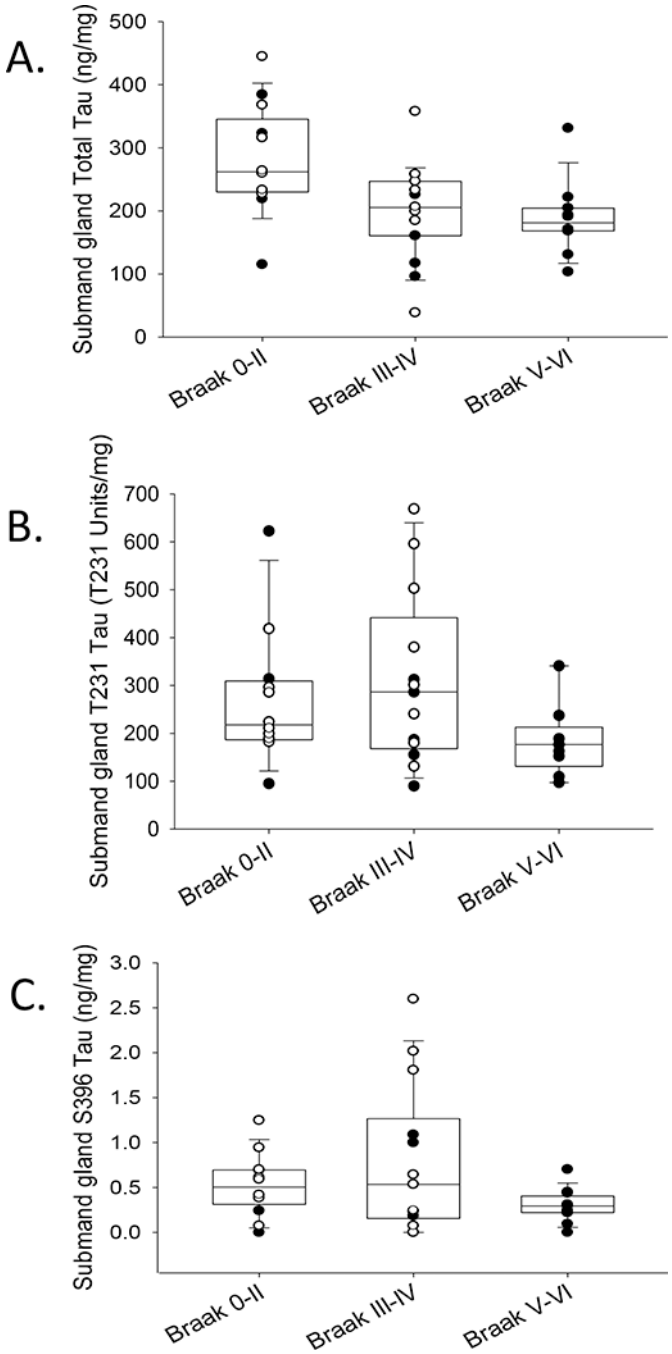


**Figure 6.**

Box and whisker plots with overlaying dot plots of ELISA measures of A) total, B) T231 and C) S396 tau species in submandibular glands across grouped Braak NFT stages (white dots = ND and black dots= AD cases). When adjusting for age, PMI, and gender there was a significant relationship with T231 (p=0.04) a marginal significant relationship with total tau levels (p=0.051) and no statistical significant relationships with S396 (p=0.162) with respect to grouped Braak NFT stage. mg refers to mg of total protein.

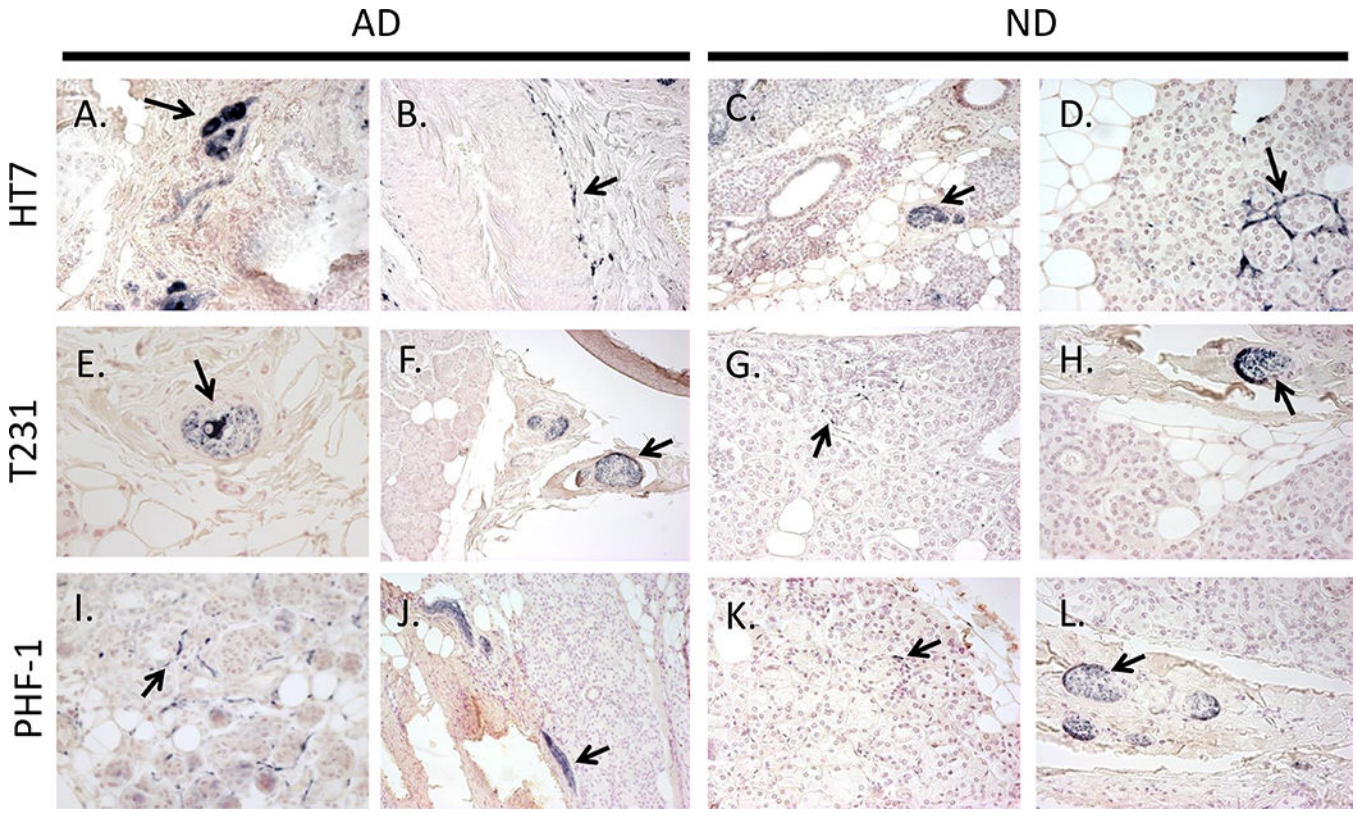


**Figure 7.**

Examples of immunoreactive HT7 (A-D), T231 (E-H), and PHF-1 (I-L) nerve elements (black arrows) within submandibular glands of AD (left) and ND (right) cases. Immunoreactive ganglion cells (A, E), nerve fibers surrounding an arteriole (B), stromal nerve fascicles (A, C, E, F, H, J, L), and nerve fibers intertwined amongst glandular acini (D, G, I, K). Photos were taken at 40x magnification, except for C, F, and J which were taken at 20x.

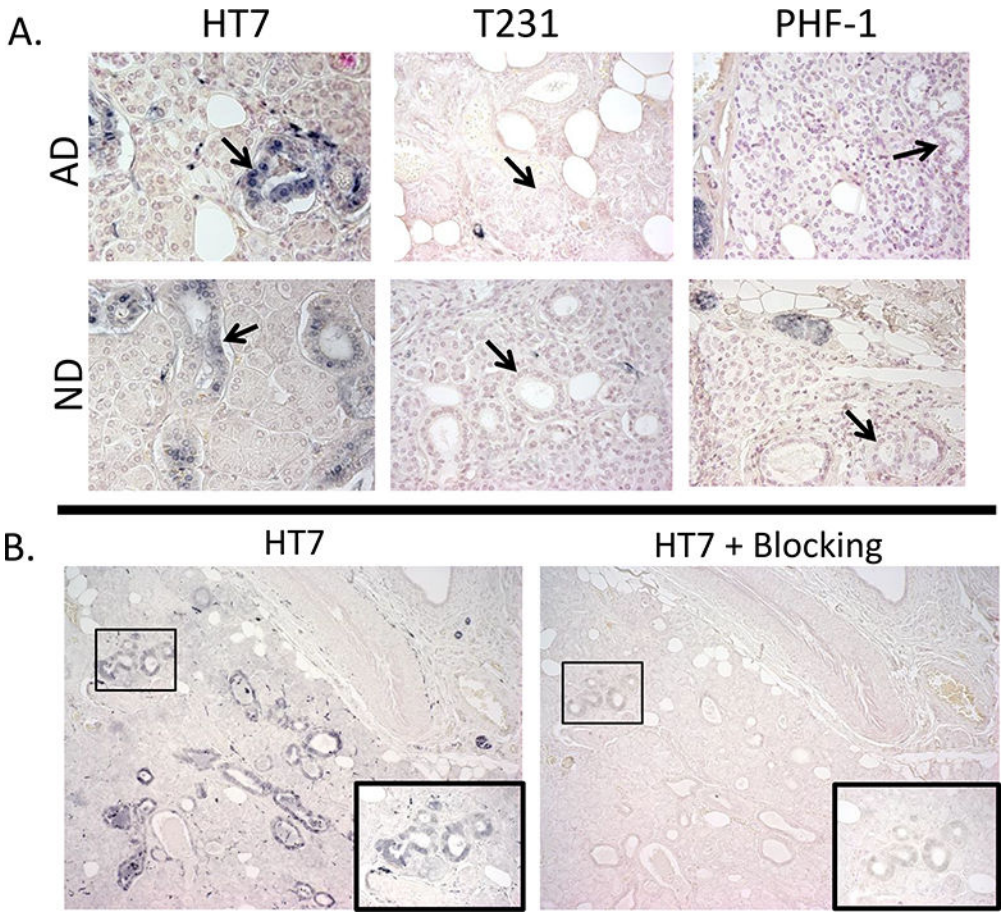


**Figure 8.**

A) Examples of simple cuboidal epithelial cell (black arrows) immunoreactivity with HT7, but not with PHF-1 or T231 within the submandibular gland of AD and ND cases; photos taken at 40x. B) Submandibular gland tissues stained with HT7 (left) and probed with HT7 and a blocking peptide (10x the concentration of HT7) directed towards the HT7 sequence (right) demonstrated diminished immunoreactivity; photos taken at 10X magnification. Images in insets show the corresponding boxed area at higher magnification.

**Table 1.**

Demographic of cases analyzed for peripheral tau.

| Case # | age at death (yrs) | gender | disease dur. (yrs) | PMI (hrs) | Braak NFT stage | ApoE genotype | diagnostic group |
|---|---|---|---|---|---|---|---|
| 1 | 90 | F | - | 2.5 | IV | 3/3 | ND |
| 2 | 85 | M | - | 12.3 | III | 2/3 | ND |
| 3 | 86 | M | 3 | 2.8 | IV | 3/3 | AD |
| 4 | 80 | F | 6 | 3.0 | V | 3/3 | AD |
| 5 | 87 | F | 5 | 3.0 | V | 3/3 | AD |
| 6 | 93 | F | 10 | 2.9 | VI | 3/3 | AD |
| 7 | 84 | M | 17 | 8.3 | V | 4/4 | AD |
| 8 | 77 | M | 6 | 2.8 | IV | 4/4 | AD |
| 9 | 82 | F | 12 | 2.5 | VI | 3/4 | AD |
| 10 | 81 | M | 2 | 3.3 | V | 3/4 | AD |
| 11 | 82 | F | 11 | 4.0 | VI | 3/3 | AD |
| 12 | 92 | F | 18 | 3.0 | V | 3/4 | AD |
| 13 | 76 | M | 3 | 3.3 | V | 3/3 | AD |
| 14 | 77 | M | 10 | 4.8 | IV | 3/3 | AD |
| 15 | 87 | M | 9 | 2.7 | V | 4/4 | AD |
| 16 | 92 | F | 5 | 2.5 | VI | 3/3 | AD |
| 17 | 86 | M | 8 | 2.3 | V | 3/4 | AD |
| 18 | 88 | F | n/a | 2.7 | IV | 3/3 | AD |

Abbreviations: PMI=post mortem interval, AD= Alzheimer's disease, Dur= duration, ND= non-demented control, NFT= neurofibrillary tangle

**Table 2.**

Demographics of Braak NFT groups for additional submandibular gland tissues.

| | Braak NFT stage | | | |
|---|---|---|---|---|
| | **0-II** | **III-IV** | **V-VI** | **P value** |
| N | 12 | 14 | 9 | n/a |
| AD:ND | 4:8 | 5:9 | 10:0 | 0.003 |
| M:F | 4:8 | 4:10 | 4:6 | 0.957 |
| age at death, yrs | 72±17.5 | 87±6.1 | 84±6.0 | 0.052 |
| PMI, hrs | 3.2±1.40 | 3.7±2.59 | 3.2±0.58 | 0.973 |
| % APOE 4 carriers | 33.3% | 35.7% | 77.8% | 0.081 |

Abbreviations: PMI=post mortem interval, AD= Alzheimer's disease, ND= non-demented control, NFT= neurofibrillary tangle.

**Table 3.**

ELISA results of total tau in the submandibular gland, liver, sigmoid colon, abdominal skin and scalp as compared to the middle frontal gyrus grey matter of the same individuals. Total tau levels are listed as average ± standard deviation.

| | ND (n=2) | AD (n=16) |
|---|---|---|
| Total tau brain levels (ng/mg total protein) | 7941 ± 237 | 7881 ± 2945 |
| Subman. Gland (% brain) | 1.72% | 1.67% |
| Ab. Skin (% brain) | 0.26% | 0.34% |
| Scalp (% brain) | 0.23% | 0.18% |
| Colon (% brain) | 0.26% | 0.33% |
| Liver (% brain) | 0.24% | 0.16% |

All percentages are listed as averages.